

Optical phase-coherent link between an optical atomic clock and 1550 nm mode-locked lasers

Kevin W. Holman, David J. Jones, Steven T. Cundiff, and Jun Ye*

JILA, National Institute of Standards and Technology and University of Colorado

Boulder, CO 80309-0440

(303)-735-3171 (Voice) 303-492-5235 (Fax) Ye@jila.colorado.edu

John B. Schlager

National Institute of Standards and Technology, Boulder, CO 80303

Erich P. Ippen

Research Laboratory of Electronics, Massachusetts Institute of Technology

Cambridge, MA 02139

Abstract: We report the lowest timing jitter and direct optical phase coherence between 1550 nm mode-locked laser sources and an 800 nm femtosecond frequency comb serving as the clockwork for an optical atomic clock.

Femtosecond (fs) optical frequency combs have made major impacts on frequency metrology and ultrafast optics [1,2]. A logical next step is to extend the spectral coverage into the 1.5 μm wavelength region, where compact, reliable, and efficient mode-locked lasers exist [3].

Frequency reference grids at these wavelengths could find applications in dense wavelength division multiplexed (DWDM) systems, photonic samplers in high-speed A/D conversion, and distribution of optical frequency standards over optical fiber networks. We report results of tight synchronization between the repetition rates and coherent phase locking of the optical carriers of the 1550 nm mode-locked laser sources and a Ti:Sapphire -based fs frequency comb, which is used as clockwork for an optical atomic clock based on a molecular iodine transition.

A phase-coherent link between mode-locked lasers requires two distinct conditions to be met [4], as shown in Fig. 1. The comb spacing of the 1550-nm source ($f_{\text{rep},1550}$) must be stabilized to the optical clock's fs comb spacing ($f_{\text{rep},775}$). Second, the combs' offset frequencies ($f_{\text{ceo},775}$ and $f_{\text{ceo},1550}$) must be phase locked together. This latter step requires spectral overlap between the two combs. The wide bandwidth optical frequency comb generated by the mode-locked fs Ti:sapphire laser is phase locked to a highly stable, iodine-based optical frequency standard [5]. The optical comb of the 1550-nm source is frequency doubled and compared against the Ti:sapphire comb at a mutually accessible spectral region to generate a heterodyne beat.

We have investigated three different types of passively mode-locked lasers in the 1550-nm region, including an erbium/ytterbium-doped waveguide laser, an erbium-doped fiber laser, and a mode-locked laser diode (MLLD). Each laser offers at least two control parameters to obtain simultaneous time synchronization and carrier phase locking. For example, stabilization through

the cavity length is a common feature for all three lasers. The carrier-envelope offset frequency ($f_{\text{ceo},1550}$) can be tuned in both waveguide and fiber lasers through control of the intensity of their pump lasers. A MLLD on the other hand can be tuned with both the injection current and the reverse bias voltage on the saturable absorber. Among the three mode-locked laser sources, the waveguide laser achieved the lowest residual timing jitter with a record-low, root-mean-square relative timing jitter of 14.4 fs integrated from 10 Hz to 375 MHz (the Nyquist frequency), owing to the laser's high-Q cavity and overall gain dynamics. Although the MLLD has a larger rms timing jitter of ~ 22 fs within the bandwidth of 1 Hz – 100 MHz, it does offer the advantage of a compact size, robust operation, and completely electrical control, along with the potential in device improvements to lower the jitter at high frequencies.

In pursuit of simultaneous synchronization and phase locking, the MLLD displays particularly interesting mode-locking dynamics and we need to understand the dependence of the MLLD comb dynamics on all of its relevant operating variables, i.e., the injection current I_d , the reverse bias voltage on the saturable absorber V_s , and the external cavity length l_c . When the value of V_s is increased, the band gap of the saturable absorber shifts to a lower energy, resulting in a larger value of refractive index, n , at the operating wavelength. A smaller band gap also leads to an increase in the band edge curvature, and so $(dn/d\omega)$ increases. Hence, the pulse group velocity decreases, leading to a reduced value of $f_{\text{rep},1550}$. The differential rates of change of n and $(dn/d\omega)$ also cause a change in $f_{\text{ceo},1550}$ as V_s increases. On the other hand, when I_d increases, the enhanced free-carrier density leads to smaller values of n and hence larger values of $f_{\text{rep},1550}$. The influence of I_d on $(dn/d\omega)$ is more complicated and is related to the wavelength and current

dependence of the linewidth enhancement factor (α) of the specific diode structure. Empirically we find that a larger I_d leads to a smaller $f_{\text{ceo},1550}$.

Since changes in V_s affect both $f_{\text{ceo},1550}$ and $f_{\text{rep},1550}$ in a similar manner, while changes in I_d cause opposite changes in $f_{\text{ceo},1550}$ and $f_{\text{rep},1550}$, we have implemented the following strategy for optimal control. Error signals associated with fluctuations of both $f_{\text{ceo},1550}$ and $f_{\text{rep},1550}$ are combined linearly with appropriate signs and gains respectively to produce two control signals, one for I_d , and the other for V_s . This process represents a simple diagonalization of a 2×2 matrix, leading to two orthogonal control loops for $f_{\text{ceo},1550}$ and $f_{\text{rep},1550}$. In addition, the piezo-activated external cavity mirror can be used to vary l_c so that a higher loop gain in the low frequency range can be implemented to control $f_{\text{ceo},1550}$. Sensitivity of the l_c change on $f_{\text{rep},1550}$ is overwhelmed by the combined action of I_d and V_s and it can be safely neglected in the overall design of the control loop.

With the implementation of the orthogonal control loop, we have achieved simultaneous stabilization of $f_{\text{ceo},1550}$ and $f_{\text{rep},1550}$ with basically no compromise in performance for either $f_{\text{ceo},1550}$ or $f_{\text{rep},1550}$, as compared to the optimized and independent single-parameter control.

Without an optimized orthogonal control, stabilization of one parameter causes a degradation of the other parameter. The MLLD repetition rate $f_{\text{rep},1550}$ is first stabilized to $f_{\text{rep},775}$ by modulating the saturable absorber with an injection microwave signal that is extracted from the iodine-based optical atomic clock. The 8th harmonic of the clock signal matches the fundamental repetition rate of the MLLD of 6.0 GHz. To improve the synchronization further (leading to lower residual timing jitter), $f_{\text{rep},1550}$, which is detected by a fast detector receiving a portion of the MLLD

optical output, is phase-sensitively compared against $(8 \times f_{\text{rep},775})$ and the resultant error signal is fed into the orthogonal control loop. To phase lock the MLLD's $f_{\text{ceo},1550}$ to that of the optical clock's fs comb, the optical output of the MLLD is first amplified by two stages of erbium-doped fiber amplifiers and then focused into a 2 cm long piece of periodically-poled Lithium-Niobate (PPLN) for efficient second harmonic generation, producing 35 μW centered at 775 nm. The frequency-doubled signal from the MLLD is then co-linearly combined with the Ti:sapphire femtosecond comb to generate a heterodyne beat $(= 2f_{\text{ceo},1550} - f_{\text{ceo},775})$. The heterodyne beat is processed by a digital phase detector against a stable radio frequency reference and the subsequent error signal is fed into the orthogonal control loop.

Figure 2 demonstrates the effect of the orthogonal control loop optimized for both $f_{\text{ceo},1550}$ and $f_{\text{rep},1550}$. The dashed line in Fig. 2(a) represents the spectral density of the residual timing jitter obtained by comparing the phase of $f_{\text{rep},1550}$ against that of $(8 \times f_{\text{rep},775})$ when the lasers are synchronized by injection of the external microwave clock signal to the saturable absorber. Any attempt to stabilize $f_{\text{ceo},1550}$ via control of V_s leads to increased timing jitter in the synchronization loop, as shown by the solid trace in Fig. 2(a). However, by maintaining the microwave injection to the saturable absorber and activating the orthogonal control loop to stabilize both $f_{\text{ceo},1550}$ and $f_{\text{rep},1550}$, the residual timing jitter is reduced by a factor of 10 within the bandwidth of the servo loop, shown by the dotted trace in Fig. 2(a). This level of performance for the synchronization loop is basically the same as if only $f_{\text{rep},1550}$ is stabilized while $f_{\text{ceo},1550}$ is left floating. Figure 2(b) illustrates the second important aspect of the orthogonal control. Three traces are shown, depicting the line shape of the heterodyne beat signal $(2f_{\text{ceo},1550} - f_{\text{ceo},775})$ under three different conditions. The top trace represents the beat signal when the MLLD is synchronized to the

Ti:sapphire laser comb via injection to the saturable absorber. When the synchronization is further improved by using only feedback on I_d , the phase error of the $f_{\text{rep},1550}$ loop (corresponding to the residual timing jitter) can be reduced by a factor of 10. However, the linewidth of the heterodyne beat, and hence $f_{\text{ceo},1550}$, is broadened. This scenario is shown by the trace in the middle of Fig. 2(b). When the orthogonal control loop is activated, not only is the $f_{\text{rep},1550}$ loop improved as shown in Fig. 2(a), but the coherence of $f_{\text{ceo},1550}$ is also improved as shown by the narrowed line shape of the bottom trace in Fig. 2(b).

Figure 3 (a) shows frequency-counting records of the beat between the MLLD and Ti:sapphire combs under locked and unlocked conditions. At 1-s gate time, the rms fluctuation (σ_{rms}) of the heterodyne beat is 1.5 MHz when $f_{\text{ceo},1550}$ is not stabilized. Under the orthogonal control condition, σ_{rms} of $(2f_{\text{ceo},1550} - f_{\text{ceo},775})$ is reduced to 3.2 mHz. By monitoring the beat error signal produced by the digital phase detector we insure that no cycles have slipped over this measurement period. Allan deviation of the stabilized beat frequency record is shown in Fig. 3 (b), determined with respect to the 1550 nm optical carrier frequency. The deviation averages down somewhere between $1/\tau$ and $1/\sqrt{\tau}$ (τ is the averaging time), indicating a mixture of white frequency and phase noise in the phase-locked loop.

We thank Dr. J. Hall for useful discussions. This work is supported by ONR, NASA, AFOSR, NIST, and NSF. K. Holman is a Hertz Foundation graduate Fellow.

References:

1. Th. Udem, R. Holzwarth, and T. Hansch, *Nature* **416**, 233 (2002).
2. S. T. Cundiff and J. Ye, *Rev. Mod. Phys.* **75**, 325 (2003).
3. D. J. Jones, K. W. Holman, M. Notcutt, J. Ye, J. Chandalia, L. Jiang, E. Ippen, and H. Yokoyama, *Opt. Lett.* **28**, 813 (2003).
4. R. K. Shelton, L.-S. Ma, H. C. Kapteyn, M. M. Murnane, J. L. Hall, and J. Ye, *Science* **293**, 1286 (2001).
5. J. Ye, L.-S. Ma, and J. L. Hall, *Phys. Rev. Lett.* **87**, 270801 (2001).

Figure Captions:

Fig. 1 Schematic diagram of simultaneous synchronization and phase locking between a 1.55- μm MLLD and a 775-nm mode-locked Ti:sapphire laser. The shaded area shows the implementation of an optical clock based on a Ti:sapphire fs comb phase-stabilized to an iodine standard. The MLLD's repetition frequency is 8 times that of the Ti:sapphire (not as shown in the figure).

Fig. 2 (a) Relative timing jitter for the synchronization loop under the conditions of (1) microwave injection to the saturable absorber (dashed trace); (2) synchronization via injection locking and phase locking via saturable absorber bias voltage (solid trace); and (3) synchronization and phase locking via orthogonalized control (dotted trace).

(b) Heterodyne beat signals between the frequency doubled MLLD and the Ti:sapphire combs under the conditions of (1) synchronization via microwave injection to the saturable absorber (top trace); (2) synchronization via injection current (I_d) servo (middle trace); and (3) synchronization and phase locking via orthogonalized control (bottom trace). The traces are offset vertically for viewing clarity.

Fig. 3 (a) Heterodyne beat recorded by a frequency counter at 1 s gate time, under no phase locking (short trace, with respect to the right vertical axis) and phase locking (long trace, with respect to the left vertical axis). (b) Allan deviation associated with the phase-locked signal.

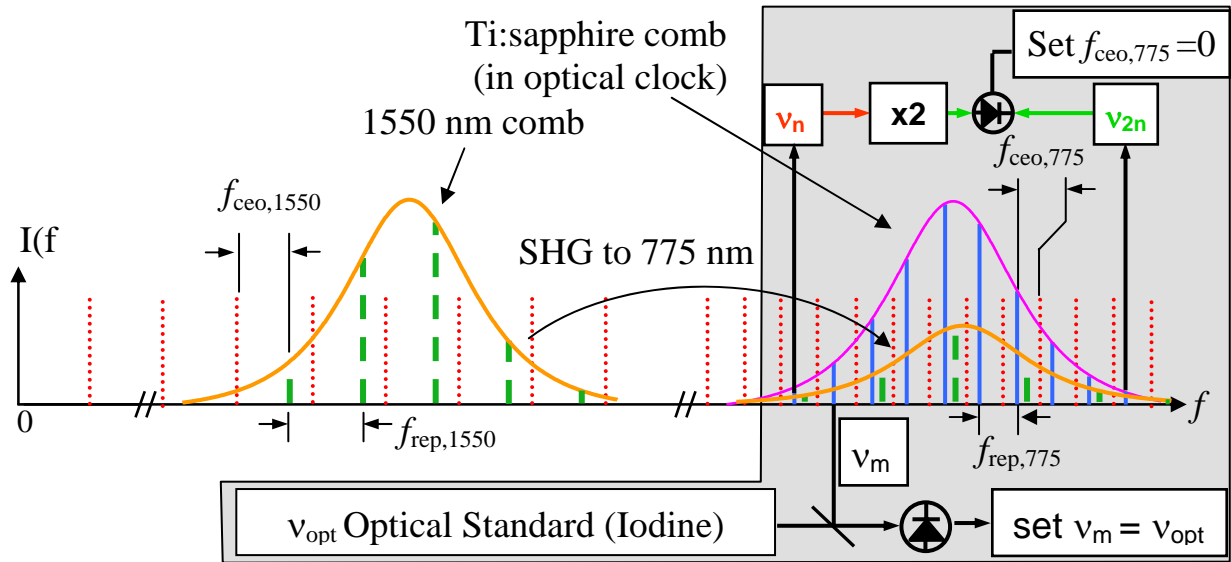


Figure 1

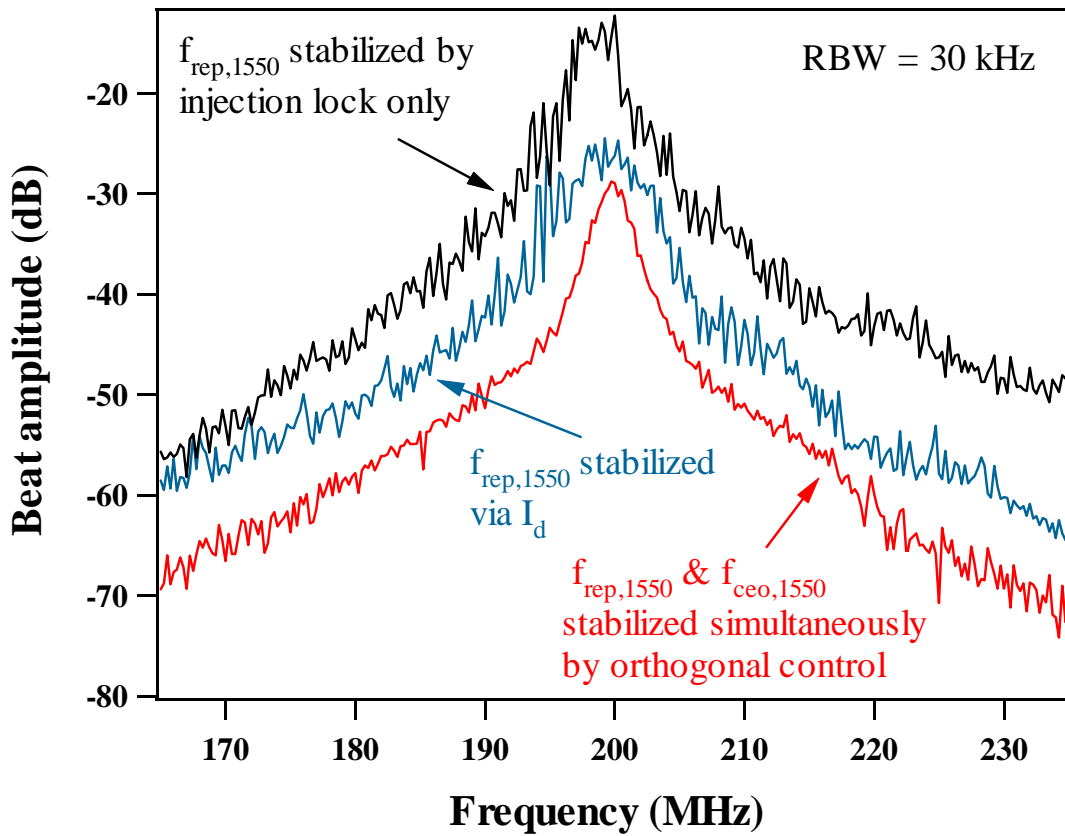
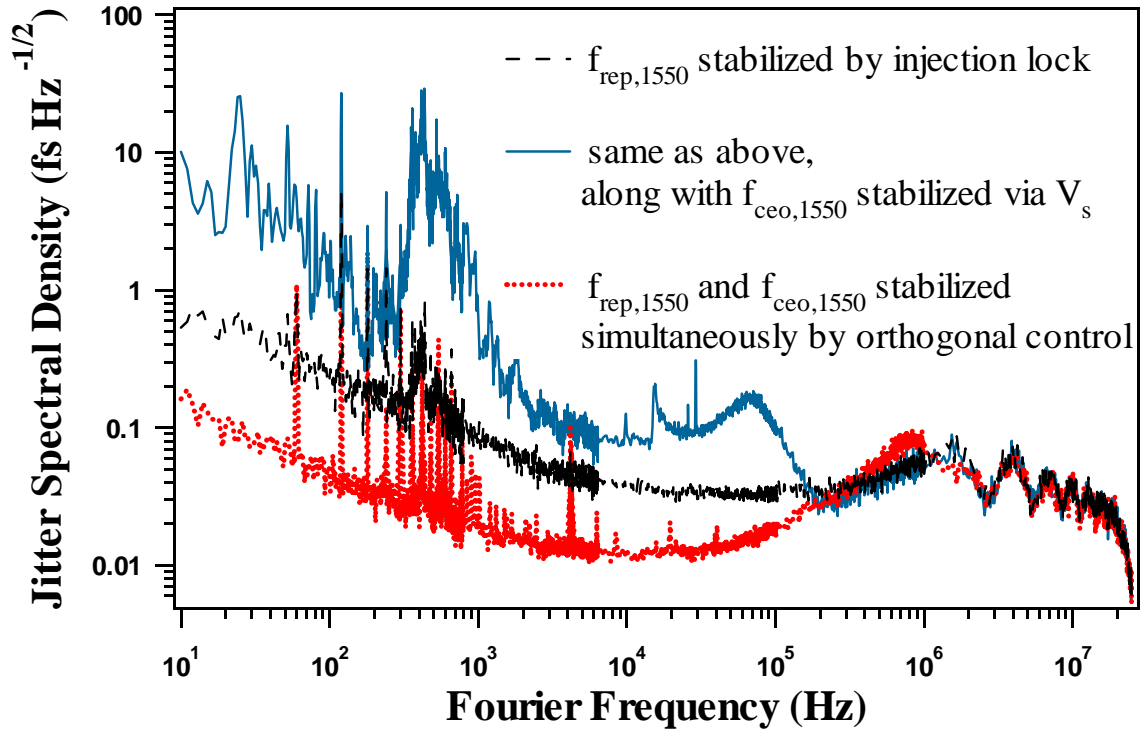


Figure 2

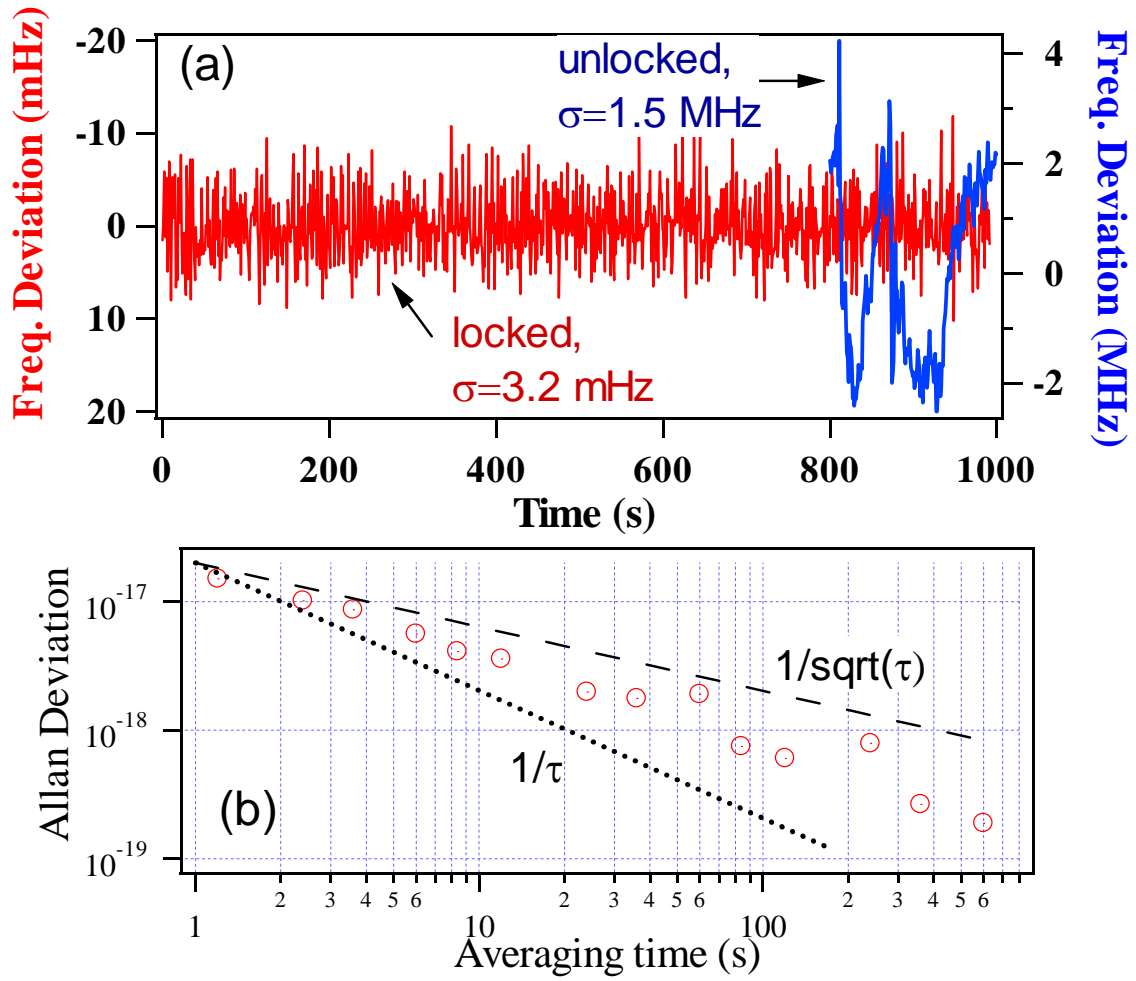


Figure 3